Roadside IoT Sensor-Based Crack Detection for Smart Roads

Fendi Ma, Gang Wang, Yilong Hui, Ruijin Sun, Changle Li, and Guoqiang Mao*
State Key Laboratory of Integrated Services Networks, Xidian University, Xi'an, 710071, China
Research Institute of Smart Transportation, Xidian University, Xi'an, 710071, China
*guoqiangmao@xidian.edu.cn

2023 IEEE 98th Vehicular Technology Conference (VTC2023-Fall) | 979-8-3503-2928-5/23/$31.00 ©2023 IEEE | DOI: 10.1109/VTC2023-Fall60731.2023.10333752

***Abstract*—The rapid development of Internet of Things (IoT) technology can significantly promote the development and deployment of smart roads, enabling efficient and reliable road information sensing and analysis. As an important part of smart roads, timely and accurate detection of road cracks can improve service life of roads and reduce road management and operating costs. In this paper, we propose a vibration-sensor-based crack detection scheme for smart roads. In this scheme, by deploying the vibration sensor on the roadside, the changes in the vibration signals caused by the vehicle passing through the range of the sensor can be collected in real time. Then, considering that the seismic waves caused by vehicle driving are mostly distributed in the low-frequency range, we perform low-pass filtering on the collected vibration signals to retain the low-frequency vibration signals. After that, in order to distinguish the crack state of the road, we extract the vibration signal features of the normal road and the cracked road in the time domain, frequency domain and time-frequency domain, respectively. Based on the extracted features, we use logistic regression (LR), support vector machine (SVM) and random forest classification (RFC) machine learning algorithms to realize road crack detection. Finally, we conduct experiments to evaluate the performance of the proposed road crack detection scheme. The experimental results verify the high accuracy of the proposed scheme, and the accuracy of LR, SVM and RFC are 93.3%, 93.3% and 96.7%, respectively.**

***Index Terms*—Internet of things, smart roads, vibration sensing, machine learning, crack detection.**

I. Introduction

With the increase in the number of cars, road conditions have received extensive attention from the global academic and industrial communities [1]. As the foundation of the transportation system, maintaining good road conditions can effectively reduce the occurrence of traffic accidents [2]. However, the repair and maintenance of traditional roads require a significant amount of manpower and substantial costs [3].

As a typical application of IoT technology, the intelligent transportation systems (ITS) composed of various sensing devices and transmission devices can provide holographic road information sensing and promote the digitization and informatization of transportation systems [4], [5].

When a vehicle is driving on the road, it means that the vehicle is exerting a certain excitation on the ground. For non-rigid terrestrial medium, this excitation will cause deformation of the terrestrial medium, and the deformation will propagate in the terrestrial medium to form vibration signals [6]. Therefore, the IoT sensors placed on the roadside will receive the vibration signals caused by the driving of the vehicle, and then upload the detected vibration signals to the cloud server. After collecting the data from a number of IoT sensors, the cloud server can analyze the vibration signals to obtain the road health status.

Based on the above principle, road crack monitoring based on the IoT sensors has been extensively studied in recent years. Zhong et al. [7] propose a Ground Penetrating Radar (GPR) based scheme to detect the defects of airport road surface. But GPR requires manual operation and the F1-measures for road crack is only 33%. Based on the vibration and sound signals induced by road vehicles, Pratic et al. [8] use four machine learning algorithms to detect road cracks. Although the final recognition accuracy is high, the paper only uses the original vibration and sound signals for detection, and does not conduct in-depth feature analysis on the vibration and sound signals. Fedele R [9] use a microphone to collect vibration and sound signals, and then use power spectrum to analyze the signal features of different damaged roads. Akanksh et al. [10] implement the detection of crack roads using different multi-class supervised machine learning techniques by collecting data from smartphone, accelerometers, gyroscopes and GPS. In [11], Takanashi et al. install vibration sensors on road shoulders. They collect vibration signals and use anomaly detection techniques to detect road cracks. However, they directly use the original vibration signal value and spectrum value as the data for anomaly detection, where the large amount of feature data increases the computational complexity of the algorithm.

From the above discussions, we can know that the current sensor-based road crack detection schemes do not consider the road crack vibration signal analysis. Therefore, in this paper, we propose a method to detect cracks on roads by installing vibration sensors on the roadside. According to the criteria for assessing road technical conditions, the transverse cracks in roads discussed in this paper belong to one type of pavement condition. Specifically, we use roadside-deployed vibration sensors to sense the vibration signals caused by vehicle driving in real time. In order to preserve as many low-frequency road vibration signals as possible, we perform low-pass filtering on the sensing signals. Then, in order to distinguish the road crack state, we extract the vibration signal features in the time domain, frequency domain and time-frequency domain, respectively. According to the extracted features, we use logistic regression (LR), support vector machine (SVM) and

979-8-3503-2928-5/23/$31.00 ©2023 IEEE

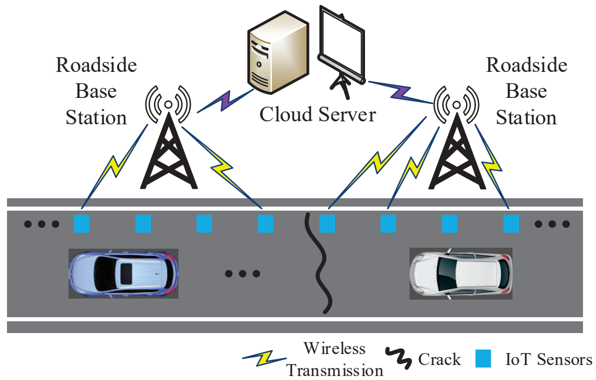

Fig. 1. Architecture diagram of smart roads crack detection system.

random forest classification (RFC) algorithms to detect road cracks and verify the effectiveness of the extracted features. Finally, we evaluate the performance of the proposed smart roads crack detection algorithm through experiments.

The remainder of this paper is organized as follows. Section II presents the system model of the proposed smart roads crack detection system. In section III, the road crack detection algorithms are described. Section IV presents the experimental results, followed by the conclusion in section V.

II. System Model

A. Scenario Description

In this section, we describe the smart roads crack detection system. As shown in Fig. 1, the system consists of roadside IoT sensors, roadside base stations and a cloud server.

Roadside IoT Sensors: The IoT sensors consist of an acceleration sensor, a microprocessor and a wireless transmission module. The acceleration sensor is AG205, which is a piezoelectric acceleration sensor. As shown in Fig. 1, the sensor is arranged along the roadside to collect the vibration signals. The microprocessor is STM32F103RCT6, which is used to control the acceleration sensor and process the data collected by the sensor. After obtaining the vehicle vibration signals, the controller uploads the vibration signals from the LoRa wireless transmission module to the roadside base station.

Roadside Base Stations: The roadside base station integrates a LoRa wireless transmission module and a 4G transmission module. The LoRa wireless transmission module is used to collect the data uploaded by the roadside IoT sensors, and the 4G transmission module repackages the uploaded data and forwards the data to the cloud server.

Cloud Server: The cloud server is used to receive the data uploaded by the 4G transmission module, and then extracts the vibration signal features in the time domain, frequency domain and time-frequency domain. Based on the extracted features, machine learning algorithm is used to detect cracks in smart roads.

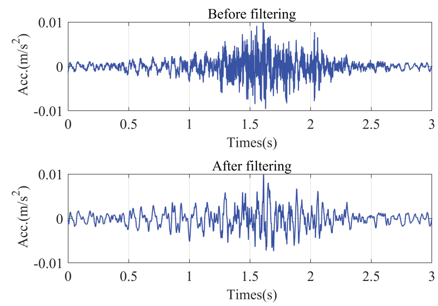

(a) Flat road

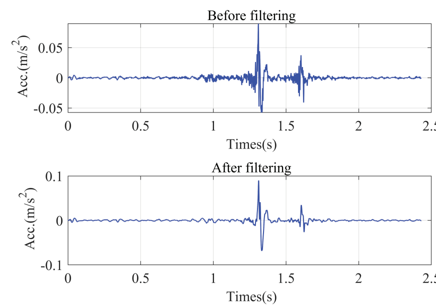

(b) Cracked road

Fig. 2. Road vibration signals.

B. Signal Progressing Model

Fig. 1 shows the architecture diagram of the smart roads crack detection system. In the system, multiple roadside IoT sensors are deployed on the roadside at equal intervals of distance D. To ensure rigid contact with the road, IoT sensors need to be embedded in the road to collect vibration signals. When a vehicle passes the detection range of the IoT sensor, the vibration signals will be collected at sampling rate f_s. In order to reduce the impact of higher-frequency sound waves such as vehicle engines and pay attention to low-frequency road vibration signals, we set up a 2-order low-pass digital filter with a cut-off frequency of 150Hz to low-pass filter the vibration signals. The vibration signals before and after filtering are shown in Fig. 2.

III. Road Crack Detection Algorithms

According to the vibration signals sensed by roadside IoT sensors, we first extract the features and then propose a road crack detection algorithm based on machine learning to detect road crack.

A. Feature Extraction

To enhance the accuracy of road crack detection, the feature selection process should prioritize significant distinctions in crack features. This section presents six features extracted from the domains of time, frequency, and time-frequency, aiming to achieve improved classification results.

1) Time Domain Features: When a vehicle traverses a cracked road, the vibration signal exhibits substantial deviations from the average, resulting in numerous spikes. Consequently, two features are extracted in the time domain: standard deviation and kurtosis factor. Specifically, the standard deviation quantifies the extent of deviation of the vibration signal from its mean value, while the kurtosis factor evaluates the presence of spikes in the vibration signal.

Standard deviation: The standard deviation of the vibration signal can be calculated by

$$\sigma = \sqrt{\frac{1}{N-1}\sum_{k=1}^{N}(x(k)-\mu)^2} \tag{1}$$

$$\mu = \sum_{k=1}^{N}\frac{x(k)}{N} \tag{2}$$

where $x(k)$ is the k-th vibration signal value, N is the length of the vibration signal, and μ is the average value of the vibration signal.

Kurtosis factor: The kurtosis factor of the vibration signal can be expressed as

$$K = \frac{\sum_{k=1}^{N}(x(k)-\mu)^4}{N\cdot\sigma^4} \tag{3}$$

2) Frequency Domain Features: Road cracks impose significant impact on vehicle travel, resulting in increased energy and power consumption. Furthermore, road damage leads to alterations in the overall road structure. Therefore, the inherent property, namely frequency will be affected. Taking these factors into account, we extract the average power as a metric for quantifying the power variation in vibration signal caused by road cracks. Additionally, the center frequency feature is employed to represent the overall shift in the natural frequency of road cracks. To calculate the power spectrum of the vibration signal, we utilize the Welch method, shown as

$$PSD(w) = \sum_{i=1}^{N/W}\frac{|X_i(w)|^2}{W} \tag{4}$$

where W is the window width of the window function, and $X_i(w)$ is the spectrum of each segment.

Average power: The average power of the vibration signal can be calculated by

$$\overline{PSD} = \frac{1}{M}\sum_{i=1}^{M}PSD(i) \tag{5}$$

where M is the index corresponding to 150 Hz of the effective frequency spectrum of the vibration signal, and $PSD(i)$ is the power value corresponding to the i-th frequency value.

Center frequency: Center frequency of the vibration signal is calculated by

$$f_c = \frac{\sum_{i=1}^{M}f_i\cdot PSD(i)}{\sum_{i=1}^{M}PSD(i)} \tag{6}$$

where f_i is the i-th frequency value.

3) Time-frequency Domain Features: The presence of road cracks induces changes in the vibration signal. To effectively analyze these changes, the wavelet transform decomposes the vibration signal into different-scale components using wavelet basis functions. Consequently, we extract the maximum energy and information entropy features from the vibration signal at various scales to capture the alterations in road structure caused by road cracks. To analyze the vibration signal in the time-frequency domain, we employ continuous wavelet transform, shown as

$$CWC(a,b) = \frac{1}{\sqrt{a}}\int x(t)\cdot\psi^*(\frac{t-b}{a})dt \tag{7}$$

$$\psi(t) = \frac{1}{\sqrt{\pi F_b}}e^{2i\pi F_c t}e^{-\frac{t^2}{F_b}} \tag{8}$$

where a is the scaling parameter of the wavelet basis function, b is the translation parameter of the wavelet basis function, and $x(t)$ is the vibration signal. ψ is the cmor wavelet basis function, ψ^* is the complex conjugate of ψ, F_b is the bandwidth factor, and F_c is the center frequency factor.

Energy: The maximum energy of the vibration signal is calculated by

$$Eng = max(Eng(a)), a = 1, 2, ...S \tag{9}$$

$$Eng(a) = \sum_{b=1}^{N}|CWC(a,b)|^2 \tag{10}$$

where S is the scale of wavelet transform.

Information Entropy: The maximum information entropy of the vibration signal can be given by

$$Ent = max(Ent(a)), a = 1, 2, ...S \tag{11}$$

$$Ent(a) = -\sum_{i=1}^{N}p_i\cdot\log_2 p_i \tag{12}$$

$$p_i = \frac{|CWC(a,i)|^2}{Eng(a)} \tag{13}$$

where p_i is the energy probability distribution of the wavelet coefficients, and $Eng(a)$ is the energy of the scale factor a.

B. Feature Normalization

There exists a significant gap between different features. For instance, the standard deviation feature is on the order of 10^{-3}, while the kurtosis factor feature ranges from 10^0 to 10^2. Therefore, it is necessary to normalize these diverse features. In the training set, we store the extracted feature values in a matrix denoted as XF to accommodate all features, XF shown as

$$XF = \begin{bmatrix} xf_{11} & xf_{12} & \dots & xf_{1j} & \dots & xf_{1L} \\ xf_{21} & xf_{22} & \dots & xf_{2j} & \dots & xf_{2L} \\ xf_{31} & xf_{32} & \dots & xf_{3j} & \dots & xf_{3L} \\ xf_{41} & xf_{42} & \dots & xf_{4j} & \dots & xf_{4L} \\ xf_{51} & xf_{52} & \dots & xf_{5j} & \dots & xf_{5L} \\ xf_{61} & xf_{62} & \dots & xf_{6j} & \dots & xf_{6L} \end{bmatrix} \tag{14}$$

where the first two rows in the matrix are the standard deviation and kurtosis factor features in the time domain, the middle two rows are the average power and center frequency features in the frequency domain, and the last two rows are the energy and information entropy features in the time-frequency domain. L is the total number of collected vibration data. For feature normalization, we use the mean variance normalization method, shown as

$$Norxf_{ij} = \frac{xf_{ij} - xf_{imean}}{xf_{istd}} \tag{15}$$

where xf_{ij} is the j-th eigenvalue of the i-th row, xf_{imean} is the mean value of the i-th row, and xf_{istd} is the standard deviation of the i-th row. After normalizing the feature mean variance, we obtain the normalized feature matrix, and then use the normalized feature matrix to train the machine learning algorithms.

C. Machine Learning Algorithms

1) Logistic Regression: Logistic regression employs the Sigmoid function $g(x) = \frac{1}{1+e^{-x}}$ as the basis for classification. The domain of the Sigmoid function is $[-\infty, +\infty]$, and its range is $[0, 1]$. Hence, this function can achieve a nonlinear mapping of data within an infinite range to the range of 0 to 1. In this paper, we leverage this property by setting $x = \theta^T F$, which transforms the Sigmoid function into the following form

$$h_\theta(F) = g(\theta^T F) = \frac{1}{1 + e^{-\theta^T F}} \tag{16}$$

According to the six features extracted by the feature extraction algorithm, the feature vector F is designed as $F = \begin{bmatrix} 1 & F_1 & F_2 & F_3 & F_4 & F_5 & F_6 \end{bmatrix}^T$. The linear coefficient of the feature is $\theta = \begin{bmatrix} \theta_0 & \theta_1 & \theta_2 & \theta_3 & \theta_4 & \theta_5 & \theta_6 \end{bmatrix}^T$, where coefficient θ_0 is the intercept term, and the other six terms determine the contribution of each feature. According to the data of the training set, the combination of Maximum likelihood estimation and random gradient descent algorithm can be used to determine the linear coefficients of the features. During the testing process, this paper only needs to obtain a feature vector from the vibration signal and apply equation (16) to obtain the value of the sigmoid function. Finally, the classification is completed by comparing it with a threshold of 0.5. Specifically, if the value is greater than 0.5, it is classified as a positive class; Otherwise, it is classified as a negative class.

2) Support Vector Machine: The intuitive understanding of a support vector machine (SVM) is to identify a hyperplane that separates positive and negative classes while satisfying the following conditions

$$\begin{cases} w^T F + b \geq +1, y = +1 \\ w^T F + b \leq -1, y = -1 \end{cases} \tag{17}$$

where $y = +1$ represents the positive class, and $y = -1$ represents the negative class. The key parameters of the hyperplane, namely the normal vectors and displacements, can be obtained by solving a convex quadratic programming problem that maximizes the margin. In the testing process, it is necessary to input the acquired vibration characteristics into the aforementioned equation (17) and determine the class of the vibration signal based on the positive and negative outcomes of the calculation.

(a) Flat road (b) Cracked road

Fig. 3. Experimental scenario.

3) Random Forest Classification: Based on the extracted features, feature recognition and classification can be achieved directly using a decision tree. However, the decision outcome of a single decision tree may be susceptible to misclassification if a particular feature data, due to noise, is erroneously classified as negative when it should be positive. To address this issue, we utilize a random forest consisting of NT ($NT \geq 2$) decision trees to make the final decision.

During the training process, each decision tree randomly selects training samples and features. This ensures a high degree of independence among different decision trees obtained through training. During testing, the random forest combines the judgment results from all decision trees. It follows the principle of majority voting, where the classification judgment result favored by the majority of decision trees is deemed the final result of the random forest.

IV. Experiment Results

In this section, we conduct experiments to evaluate the performance of the proposed road crack detection scheme.

A. Experimental Setup

As shown in Figure 3, the test scenario comprises a two-way, two-lane road, where the width of each lane is 3.5m. In this setup, we focus on the detection of cracks within a single lane. The vehicles traversing the road primarily consist of sedans and SUVs, with speeds ranging from 20 km/h to 60 km/h. The crack detection system utilizes a sensing device to collect data, with roadside base stations serving as data transfer stations for data uploading. The cloud server performs crack detection based on the data uploaded by the base stations.

During the experiment, the sampling frequency of the vibration signals is set to 1 kHz. The distance (D) is set to 10m. The Blackman window is employed as the window function for power spectral density, with a size of 100. The cmor wavelet is chosen as the wavelet base function, with a bandwidth of 5Hz and a center frequency of 0.8Hz. A total of 100 data sets are collected for each of the two types of roads, which are divided into a training set and a test set in a ratio of 7:3. The experimental parameters are summarized in Table I.

B. Experimental Results and Discussions

In this subsection, we apply the proposed road crack detection algorithms based on different features to evaluate the

TABLE I
PARAMETERS SETUP

Par.	Value	Description
f_s	1kHz	Sampling frequency
D	10m	Distance between two sensors
TH	0.006	Vehicle signal threshold
Win	200	Sliding window size
th	0.00063	Background noise threshold
W	100	Width of Blackman window
F_b	5Hz	Bandwidth of cmor wavelet
F_c	0.8Hz	Center frequency of cmor wavelet
S	512	Maximum scale of wavelet transform
L	140	Training set samples
NT	100	The number of decision trees

crack detection performance using the accuracy and F1-score indices. The accuracy is expressed as

$$Acc = \frac{TP+TN}{TP+TN+FP+FN} \tag{18}$$

where TP, TN, FP and FN represent true positive, true negative, false positive, and false negative predictions. The above parameters are obtained by comparing the actual labels with the labels predicted by the three machine learning algorithms.

F1-score is used to balance the precision and recall metrics, where a higher value indicates higher precision and recall of the algorithm's identification. It can be calculated by

$$F1-score = 2\cdot\frac{Recall\cdot Precision}{Recall+Precision} \tag{19}$$

where $Precision$ represents the precision rate, which is defined as the proportion of correctly identified positive samples among all the positive samples. $Recall$ represents the recall rate, which is the proportion of correctly identified positive samples among all actual positive samples. The expressions of $Precision$ and $Recall$ can be given by

$$Precision = \frac{TP}{TP+FP} \tag{20}$$

$$Recall = \frac{TP}{TP+FN} \tag{21}$$

Based on (18) and (19), we analyze the results of crack identification when different domain features are used individually and in combinations.

Furthermore, in order to differentiate the importance of different features in classification, for LR and SVM algorithms, this paper separately trained road surface data using the six features and then calculated the detection accuracy of individual features on cracked road surfaces to evaluate their importance. In contrast, RFC algorithm directly obtains feature importance as it records the entropy of classification nodes during decision tree classification. Figure 4 presents the importance histogram for classification and recognition using different features. When utilizing the RFC algorithm for crack detection, the kurtosis factor in the time domain holds the highest importance.

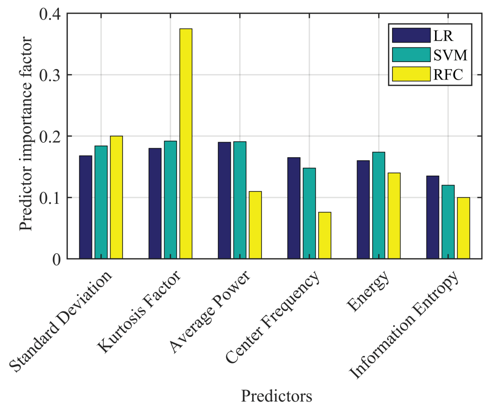

Fig. 4. Feature importance.

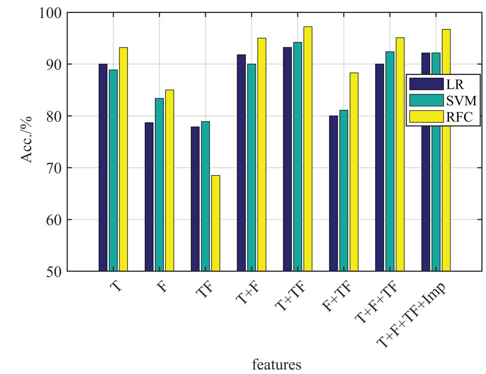

Fig. 5. Classification accuracy Note: T: time domain feature, F: frequency domain feature, TF: time-frequency domain feature, IMP: weighted feature.

Figure 5 illustrates the crack detection accuracy achieved by combining different features. As depicted in Figure 5, when utilizing individual domain features for detection, the time domain features exhibit the highest detection accuracy, reaching up to 90%. When employing pairwise combinations of domain features, merging time domain features leads to a detection accuracy equal to or greater than 90%. The highest detection accuracy using the combination of all three domains with RFC is 95%. Considering the feature importance shown in Figure 4, we reassign weights to the features using the following equation

$$w_i = \frac{IMP_i}{\sum\limits_{j=1}^{6} IMP_j}, \quad i = 1,2,\ldots,6 \tag{22}$$

where, w_i represents the feature weight, and IMP_i denotes the feature importance factor. After reassigning the weights to the features, the accuracy of the detection based on LR and RFC improves, resulting in a detection accuracy of 96.7% for RFC.

In Figure 6, for the analysis of F-scores on crack road surfaces, similar results can be obtained as the accuracy rate of crack detection. As shown in Fig. 6, the highest F-score can be achieved when using time-domain features

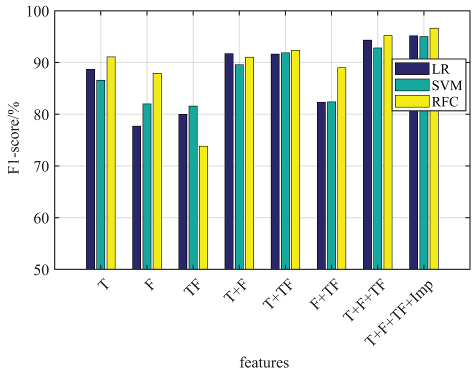

Fig. 6. Classification F1-score Note: T: time domain feature, F: frequency domain feature, TF: time-frequency domain feature, IMP: weighted feature.

alone for detection. When combining pairwise features, the F-score is significantly improved when time-domain features are included in the classification. Using a combination of three-domain features for classification, the F-score reaches 94.9%. Furthermore, after feature weight allocation, the F-scores of the three classification algorithms can be improved by 1.3%, 1.8%, and 1.7% respectively.

Based on the above analysis, when using features extracted from three domains for road crack detection, the accuracy rate and F-score of the three machine learning algorithms are higher compared to using features individually or in pairwise combinations. Additionally, by reallocating feature weights, the detection accuracy is further improved. Among the three machine learning algorithms, the RFC algorithm demonstrates the best performance, achieving an accuracy rate of 96.7% and an F-score of 96.4% for crack road surface detection.

TABLE II
PERFORMANCE COMPARISON OF DIFFERENT ROAD CRACK DETECTION METHODS

	Video Image-based Method [12]	GPR Method [7]	In-Vehicle Sensor-based Method [10]	Roadside Sensor-based Method [11]	The proposal (RFC)
Accuracy	87%	33%	61.10%	94.90%	96.70%
Computation Time	0.197s (GPU)	*	0.0992s	0.15s	0.061s

Furthermore, we compare our scheme with different sensor-based detection methods, including video image-based method, GPR (Ground Penetrating Radar) method, and IoT sensor-based method. Table II presents the comparison results, where * indicates that the detection accuracy was not provided in the literature. The detection accuracy of the proposed algorithm in this paper is comparable to other algorithms. In terms of computation time, the in-vehicle sensor-based method [10] extracts a large number of features such as standard deviation and energy in the time and frequency domains. The overall computation time for the entire algorithm is 0.0992s, indicating a significant computational load. On the other hand, the proposed crack detection algorithm focuses on the analysis of vehicle vibration signals caused by vehicle motion, resulting in a significant reduction in computation time.

V. CONCLUSION

In this paper, we have proposed a smart roads crack detection scheme based on IoT sensors. In the scheme, we have performed low-pass filtering on the vibration signals collected by the vibration sensor to remove the background noise such as higher-frequency sound waves, and retained the low-frequency road vibration information. In addition, we have extracted vibration signal features in time, frequency and time-frequency domains, and used different machine learning algorithms to detect road cracks. The experimental results have shown that the accuracy of LR, SVM and RFC are 93.3%, 93.3% and 96.7%, respectively. For future work, we plan to further improve the performance of the proposed crack detection scheme by considering the types of vehicles (i.e. trucks, vans, trolleys, etc.).

ACKNOWLEDGEMENT

This research is supported by NSFC grant, Grant number: U21A20446.

REFERENCES

[1] M. A. Hassan, R. Javed, F. Granelli, X. Gen, M. Rizwan, S. H. Ali, H. Junaid, S. Ullah *et al.*, "Intelligent transportation systems in smart city: a systematic survey," in *2023 International Conference on Robotics and Automation in Industry (ICRAI)*. IEEE, 2023, pp. 1–9.

[2] F. Guo, Y. Qian, J. Liu, and H. Yu, "Pavement crack detection based on transformer network," *Automation in Construction*, vol. 145, p. 104646, 2023.

[3] P. Wang, P. Liu, C. Wang, A. Wang, H. Guan, S. Li, and X. Xia, "Optimal dynamic investment allocation on construction of intelligent transportation infrastructure and road maintenance with environmental costs," *Journal of Cleaner Production*, vol. 284, p. 124786, 2021.

[4] Y. Cui and D. Lei, "Design of highway intelligent transportation system based on the internet of things and artificial intelligence," *IEEE Access*, 2023.

[5] G. Mao, Y. Hui, X. Ren, C. Li, and Y. Shao, "The internet of things for smart roads: A road map from present to future road infrastructure," *IEEE Intelligent Transportation Systems Magazine*, vol. 14, no. 6, pp. 66–76, 2021.

[6] D. Yang, W. Duan, G. Xuan, L. Hou, Z. Zhang, M. Song, and J. Zhao, "Self-powered long-life microsystem for vibration sensing and target recognition," *Sensors*, vol. 22, no. 24, p. 9594, 2022.

[7] H. Li, N. Li, R. Wu, H. Wang, Z. Gui, and D. Song, "Gpr-rcnn: An algorithm of subsurface defect detection for airport runway based on gpr," *IEEE Robotics and Automation Letters*, vol. 6, no. 2, pp. 3001–3008, 2021.

[8] F. G. Praticò, R. Fedele, V. Naumov, and T. Sauer, "Detection and monitoring of bottom-up cracks in road pavement using a machine-learning approach," *Algorithms*, vol. 13, no. 4, p. 81, 2020.

[9] R. Fedele, "Smart road infrastructures through vibro-acoustic signature analyses," in *INTERNATIONAL SYMPOSIUM: New Metropolitan Perspectives*. Springer, 2020, pp. 1481–1490.

[10] A. Basavaraju, J. Du, F. Zhou, and J. Ji, "A machine learning approach to road surface anomaly assessment using smartphone sensors," *IEEE Sensors Journal*, vol. 20, no. 5, pp. 2635–2647, 2019.

[11] M. Takanashi, Y. Ishii, S.-i. Sato, N. Sano, and K. Sanda, "Road-deterioration detection using road vibration data with machine-learning approach," in *2020 IEEE International Conference on Prognostics and Health Management (ICPHM)*. IEEE, 2020, pp. 1–7.

[12] Q. Zou, Z. Zhang, Q. Li, X. Qi, Q. Wang, and S. Wang, "Deepcrack: Learning hierarchical convolutional features for crack detection," *IEEE transactions on image processing*, vol. 28, no. 3, pp. 1498–1512, 2018.